PHYSICAL REVIEW B VOLUME 24, NUMBER 4 15 AUGUST 1981

Thermodynamic properties of fcc metals at high temperatures

Rosemary A. MacDonald
National Bureau of Standards, Washington, D.C. 20234

William M. MacDonald
Department of Physics and Astronomy, University of Maryland, College Park, Maryland 20742

(Received 30 March 1981)

We have carried out an exact and consistent calculation of the thermodynamic properties of monatomic fcc crystals at high temperatures. These properties are obtained from the Helmholtz free energy of the crystal $F(V,T)$ by means of the appropriate thermodynamic relations. It is crucial to the success of the calculation that we have been able to obtain the *volume* dependence of the free energy. $F(V,T)$ includes the static lattice energy and the vibrational contributions from the harmonic and lowest-order (cubic and quartic) anharmonic terms in perturbation theory evaluated in the high-temperature limit. The atoms interact via an effective nearest-neighbor central-force potential $\phi(r)$. We have calculated the specific heat at constant volume and at constant pressure, the thermal expansion, the coefficient of linear expansion, the isothermal and adiabatic bulk moduli, and the Grüneisen parameter for the following fcc metals: Cu, Ag, Ca, Sr, Al, Pb, and Ni. Good agreement with experiment is obtained in all cases. We discuss the implications of these results for further studies of the properties of metals.

I. INTRODUCTION

The evaluation of lattice dynamical theory by comparison with experiment is fraught with inconsistencies and uncertainties in the well-studied and supposedly clear-cut case of the equilibrium thermodynamic properties of solids.[1-4] The basic problem is that theory most readily deals with the system at constant volume whereas, experimentally, it is at constant pressure. Moreover, the theory is customarily expressed in terms of the volume at absolute zero V_0, the unperturbed state in perturbation theory, instead of the equilbrium volume $V(T)$ at which the experiment is performed. Uncertainties creep in through the process of adjusting for the difference between V_0 and $V(T)$. While it is perfectly straightforward, in terms of thermodynamic relationships, to convert from constant pressure to constant volume, it is not straightforward in practice. This fact has been demonstrated in a recent study of the specific heat of aluminum by Shukla and Plint.[5] They set forth the procedure clearly and consistently, but uncertainties arise in its execution, particularly in the step converting C_V, the specific heat at constant volume $V(T)$ to that at volume V_0. Not only does one need to know the equation of state accurately, but also other experimental quantities enter that are not well known, e.g., derivatives of the bulk modulus. Add to this uncertainties regarding the electronic and vacancy contributions to the specific heat and one no longer has a reliable test of the theory.

In the work we shall report here, we have been able to improve the theoretical side of things considerably using a monatomic fcc crystal model with nearest-neighbor central-force interactions between atoms. This breakthrough results from Shukla's calculations[6,7] of the lattice sums needed to obtain the Helmholtz free energy as a function of temperature *and* volume, $F(V,T)$. After calculating $F(V,T)$ for the model lattice in the high-temperature limit ($T > \Theta_D$, the Debye temperature), it is then simple to apply the appropriate thermodynamic relations and obtain the properties of interest. Our preliminary calculations of the thermal expansion of fcc metals[7] were initiated for a different purpose but they were sufficiently encouraging to make further tests of the theory essential, for if the other thermodynamic properties are well represented by this simple nearest-neighbor model, then we need to understand why this is so. This model potential is certainly very different from the long-range oscillatory potentials obtained from pseudopotential theory, which have met with success in the simple metals.[8,9]

We have calculated the lattice contribution to C_V and C_P, the isothermal and adiabatic bulk moduli, B_T and B_S, respectively, the thermal expansion ϵ, and the coefficient of linear expansion α for the following fcc metals: Cu, Ag, Ca, Sr, Al, Pb, and Ni. These results represent the first exact and consistent lattice dynamical calculation of the thermodynamic properties of a model lattice in the high-temperature limit. There still remains the problem of the electron contribution to these properties and, at temperatures close to the melting point, the contribution of vacancies. We estimate these contributions wherever possible, but this is the weak link in our comparison with experimental data—except in those cases

where no data exist. In Sec. II we outline the theory we have used in these calculations, in Sec. III we present the results, and in Sec. IV we discuss the usefulness of this model for fcc metals in practice and its implications for the theory of metals in the crystalline state.

II. THEORY

A. Free energy and thermodynamic relations

The Helmholtz free energy of the crystal $F(V, T)$ is made up of the static lattice energy and the harmonic and the lowest-order (cubic and quartic) anharmonic terms of lattice dynamical perturbation theory.[10,11] Shukla[6] has shown that, for a nearest-neighbor central-force model of a monatomic fcc crystal in the high-temperature limit, the various contributions to the free energy can be expressed in terms of the pair potential $\phi(r)$, where r is the nearest-neighbor separation, its derivatives with respect to r, and dimensionless Brillouin-zone sums S_j, which are functions of a parameter a_1 defined by

$$a_1 = \frac{\phi'(r)/r}{\phi''(r) - \phi'(r)/r}. \tag{1}$$

Thus the whole dependence of the Brillouin-zone sums on volume enters through the parameter $a_1 = a_1(r)$. This volume dependence was taken into account for the first time in our preliminary study of thermal expansion[7] and it was shown to be important. The full expression for $F(r, T)$ is given there [Ref. 7, Eqs. (2–9)]. Here we just indicate the volume and temperature dependence of the various contributions,

$$F(r, T) = 3N\left(\frac{F_1(r)}{kT} + F_2(r) + F_3(r)kT + F_4(r)(kT)^2 - kT\ln kT\right), \tag{2}$$

where the $F_i(r)$ are simply related to the functions defined in Ref. 7. Terms 1, 3, and 5 represent the harmonic contribution to the free energy, term 2 represents the static lattice energy plus the temperature-independent anharmonic contribution, and term 4 represents the temperature-dependent anharmonic contribution.

The thermodynamic properties of interest are given by the following relations.

(i) Thermal expansion $\epsilon(T)$:

$$\epsilon(T) = r(T)/r(293) - 1, \tag{3}$$

where we have chosen the pair separation at $T = 293$ K to be the reference length.

(ii) Coefficient of linear expansion $\alpha(T)$:

$$\alpha(T) = \frac{1}{r(T)}\left(\frac{dr}{dT}\right)_P. \tag{4}$$

We caution that in experimental data[12,13] α is often defined as

$$\alpha(T) = \frac{1}{r(T_c)}\left(\frac{dr}{dT}\right)_P, \tag{4'}$$

where T_c is the reference temperature, so that care must be taken when using experimental values in thermodynamic relationships.

(iii) Specific heat at constant volume C_V:

$$C_V = -T\left(\frac{\partial^2 F}{\partial T^2}\right)_V, \tag{5}$$

or, from Eq. (2),

$$C_V = 3R\left(1 - \frac{2F_1(r)}{(kT)^2} - 2F_4(r)kT\right). \tag{6}$$

(iv) Isothermal bulk modulus B_T:

$$B_T = V\left(\frac{\partial^2 F}{\partial V^2}\right)_T = \frac{\sqrt{2}}{9r(T)}F''(r, T), \tag{7}$$

where $F''(r, T)$ is the second derivative of $F(r, T)$ with respect to r at constant temperature.

(v) The specific heat at constant pressure C_P:

$$\begin{aligned} C_P &= C_V + 9\alpha^2(T)v(T)B_T T, \\ &= C_V + \tfrac{9}{2}N\alpha^2(T)r^3(T)B_T T. \end{aligned} \tag{8}$$

(vi) The adiabatic bulk modulus B_S:

$$B_S = \frac{C_P}{C_V}B_T. \tag{9}$$

(vii) The Grüneisen parameter γ:

$$\gamma = \frac{3\alpha V B_T}{C_V}. \tag{10}$$

In the remainder of this section we outline the procedure used to obtain the various derivatives that enter these relationships and give such details of the Brillouin-zone sums and interatomic potential as are needed for numerical evaluation of the thermodynamic properties.

B. Differentiation method

The equilibrium nearest-neighbor separation $r(T)$ is determined from the minimization equation

$$F'(r, T) = 0, \tag{11}$$

by iterative application of

$$\delta r = -F'(r,T)/F''(r,T)\,. \tag{12}$$

The coefficient of linear expansion $\alpha(T)$ requires, further, the differentiation of $r(T)$ with respect to T. All these derivatives, $F'(r,T)$, $F''(r,T)$, and dr/dT, were obtained from a five-point numerical differentiation formula[14] using an interval of 0.001. Change of the interval by a factor of 10 did not alter the results.

C. Brillouin-zone sums

The Brillouin-zone sums $S_j(a_1)$ which enter the $F_i(r)$ in Eq. (2), have been computed by Shukla[6,7] for values of a_1 in the range $-0.1 \leq a_1 \leq 0.1$. In order to evaluate the $S_j(a_1)$ at any value of a_1 in this range, and hence at the required value of r, we fitted Shukla's values to 6th-order polynomials or exponential polynomials, depending upon whether the sum had zero value or not within this range. A table of the least-squares coefficients for such fits is given in Ref. 7. These fits reproduce the numerical values of the $S_j(a_1)$ to better than 1 part in 10^3.

D. Modified Morse potential

The pair potential $\phi(r)$ and its derivatives appear explicitly in the functions $F_i(r)$ and also implicitly through a_1 in the functions $S_j(a_1)$. For the calculations in Ref. 7, we used a simple Morse potential fitted to the sublimation energy and Debye temperature of the metal concerned. It was also assumed that, at absolute zero, the nearest neighbor was situated at r_0, the minimum of the potential well, i.e., $r_0 = r(0)$ is determined by the lattice constant at 0 K. However, we noted there that $\phi''(r)$ was largely responsible for the slope of the computed $\epsilon(T)$ curves and that some adjustment of the curvature of the potential might give better agreement between $\epsilon(T)$ and experiment than we had obtained. To this end we have modified the potential as follows

$$\phi(r) = \frac{D_0}{1-2b}\left(e^{-2a(r-r_0)\sqrt{b}} - 2be^{-a(r-r_0)/\sqrt{b}}\right). \tag{13}$$

The values of the parameters D_0 and a are unaltered by this modification of the potential since both $\phi(r)$ and $\phi''(r)$ are independent of b, and hence identical to the Morse potential, when $r = r_0$. The parameter b has been determined during the course of the calculation for each metal by requiring that $\epsilon(T)$ fits the experimental results in the neighborhood of the Debye temperature. The usual form for the Morse potential is obtained when $b = 1$. This simple adjustment to the curvature of the potential for $r \neq r_0$ has the desired effect of bringing the results into good agreement with experiment, as we shall see in the next section.

III. RESULTS

A. Thermal expansion

We have carried out the calculations described in Sec. II for the following fcc metals: Cu, Ag, Ca, Sr, Al, Pb, and Ni. The thermal expansion of these metals has been well studied over quite a wide temperature range in most cases,[12,13] so we are able to match the computed $\epsilon(T)$ [see Eq. (3)] to experiment at the lower end of the temperature range and thus determine b. Table I lists the values of the potential parameters used in these calculations. Values of r_0 are taken from Varshni and Bloore[15] except in the case of lead, where we have used the value of Bolling quoted in Ref. 10, D_0 is obtained from the sublimation energies given by Seitz,[16] and a is obtained from Θ_D (see Ref. 7). We also list here the values of Θ_D and melting temperature[12] T_m (or, in the case of Ca and Sr, the phase transition temperature), to indicate the limits of the temperature range to which this theory is applicable.

In Figs. 1 and 2 we compare the computed $\epsilon(T)$ with experiment. In each case there is excellent

TABLE I. Parameters in calculation: Morse potential parameters, r_0 (Ref. 15), a, D_0 (Ref. 16), and b (see text); Debye temperature Θ_D and melting or phase transition (*) temperature, T_M (Ref. 12), coefficient of electron specific heat σ_0 (Ref. 26), and M' (see text).

	r_0 (Å)	a (Å^{-1})	D_0 (10^{-19} J)	b	Θ_D (K)	T_M (K)	σ_0 (10^{-4} J/mol K^2)	M'
Cu	2.5471	1.1857	0.9403	2.265	342	1356	6.945	1.391
Ag	2.8765	1.1255	0.7874	2.3	228	1234	6.276	0.986
Ca	3.9264	0.8380	0.5535	1.0	234	720*	29.999	2.529
Sr	4.2804	0.7867	0.5442	1.0	147	830*	36.401	2.582
Al	2.8485	1.1611	0.6369	2.5	423	933	13.389	2.144
Pb	3.4779	0.7776	0.5500	1.5	102	600	31.380	3.371
Ni	2.4849	1.3909	0.9843	2.4	427	1726	70.291	14.793

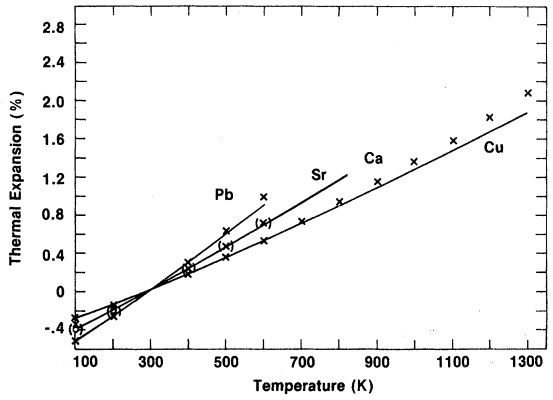

FIG. 1. Thermal expansion $\epsilon(T)$ of copper, lead, calcium, and strontium. Theory: ——, experiment: Cu (Ref. 13), ×; Pb (Ref. 12), ×; Ca (Ref. 12), ×; and Sr (Ref. 12), ○. In all figures, parentheses ( ) denote provisional values.

agreement over quite a large range of temperature. As T_m is approached, the experimental values increase more rapidly than $\epsilon(T)$. This is to be expected since we have not taken vacancies into account. Our calculation effectively determines the lattice parameter rather than the lattice dilation. However, except in the case of aluminum,[17] the difference between these two quantities is too small to be discernible on the scale of Figs. 1 and 2. Clearly, the treatment of vacancies in the high-temperature lattice needs further study.

The difference between $\epsilon(T)$ and experiment will obviously be enhanced in the coefficient of linear expansion $\alpha(T)$ as can be seen in Figs. 3 and 4. We note that none of the $\alpha(T)$ curves are in as good agreement with experiment as one would expect, judging from the $\epsilon(T)$ curves. However, the experimental values[12,13] have been obtained by differentiation of a third-order polynomial fitted

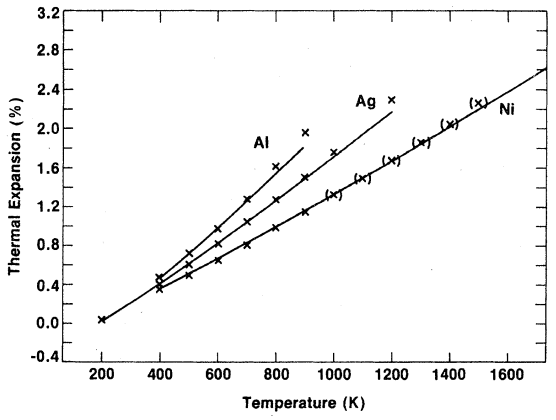

FIG. 2. Thermal expansion $\epsilon(T)$ of silver, aluminum, and nickel. Theory: ——. Experiment (Ref. 12): ×.

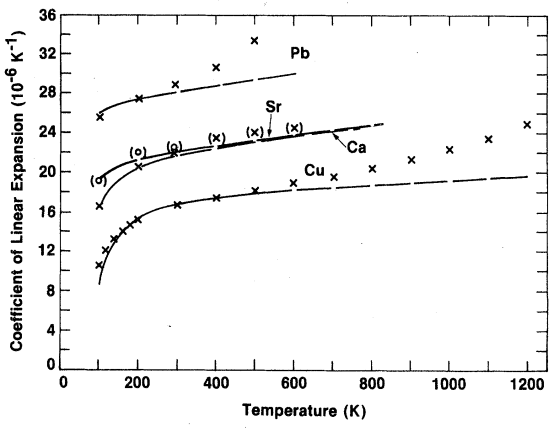

FIG. 3. Coefficient of linear expansion $\alpha(T)$ of copper, lead, calcium, and strontium. Theory: ——. Experiment: Cu (Ref. 13), ×; Pb (Ref. 12), ×; Ca (Ref. 12), ×; and Sr (Ref. 12), ○.

to the experimental thermal-expansion data, a procedure which can be quite unreliable. For this reason, we stand by our values of $\alpha(T)$ in the region where $\epsilon(T)$ agrees with experiment.

B. Bulk modulus

The lattice contribution to the bulk moduli [Eqs. (7) and (9)] is shown in Figs. 5–10. In all cases, the computed curves lie well below the experimental values.[18-22] This is to be expected since we have taken no account of electrons in our model and they are known to have a substantial effect on the compressibility of metals. We can make a rough estimate of this effect in the same spirit as we treat the electron contribution to the specific heat, viz., by means of free-electron theory.[23] For zN electrons in a volume V the free energy

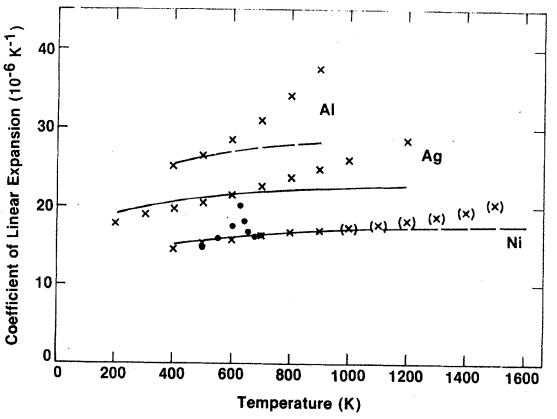

FIG. 4. Coefficient of linear expansion $\alpha(T)$ of silver, aluminum, and nickel. Theory: ——. Experiment (Ref. 12): ×. Additional data for Ni, ●, have been supplied by R. K. Kirby (private communication).

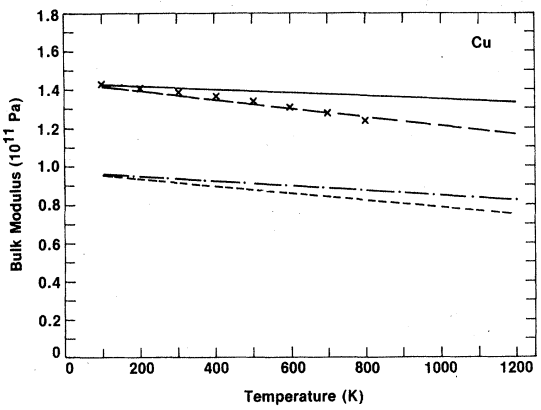

FIG. 5. Bulk moduli of copper. Lattice contribution, B_T^l, ---; B_S^l −·−; lattice plus electron contribution, B_T, ——; B_S ——. Experiment (Ref. 18): ×. Units are 10^{11} Pa for all bulk moduli.

is given by

$$F^{el} = \tfrac{3}{5} z N \zeta_{00} \left[1 - \frac{5}{12} \left(\frac{\pi k T}{\zeta_{00}} \right)^2 \right], \tag{14}$$

where z is the number of electrons per atom, ζ_{00}, the Fermi energy at $T = 0$ K, is related to the volume by

$$\zeta_{00} = \frac{1}{2m^*} \left(\frac{3h^3 N}{8\pi} \right)^{2/3} \left(\frac{z}{V} \right)^{2/3}, \tag{15}$$

m^* is the effective mass of the electrons, and h is Planck's constant. From these two relations and Eqs. 5 and 7, we obtain the expressions for the electronic contribution to the isothermal bulk modulus and specific heat, respectively,

$$B_T^{el} = \tfrac{2}{3} z \frac{N}{V} \zeta_{00} \left[1 + \frac{\pi^2}{12} \left(\frac{kT}{\zeta_{00}} \right)^2 \right] \tag{16}$$

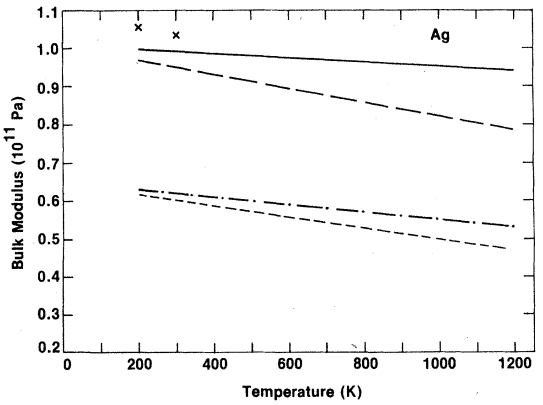

FIG. 6. Bulk moduli of silver. Lattice contribution, B_T^l, ---; B_S^l, −·−; lattice plus electron contribution, B_T, ——, B_S ——. Experiment (Ref. 19): ×.

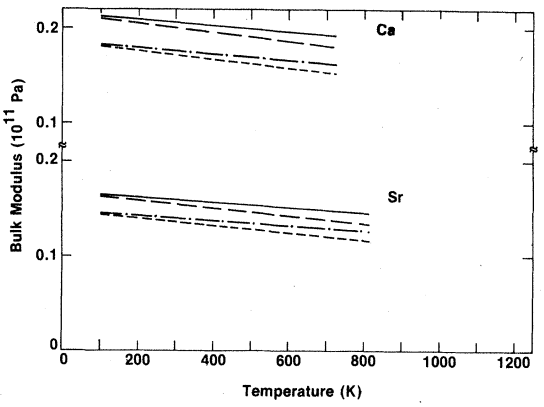

FIG. 7. Bulk moduli of calcium and strontium. Lattice contribution, B_T^l, ---; B_S^l, −·−; lattice plus electron contribution, B_T, ——; B_S, ——. No experimental values available. Note that ordinate is broken.

and

$$C_V^{el} = \frac{\pi^2}{2} z R \frac{kT}{\zeta_{00}} \equiv \sigma_0 T , \tag{17}$$

where σ_0 is the low-temperature coefficient of specific heat. We shall neglect the second term in Eq. (16) since $kT/\zeta_{00} \ll 1$ in all the metals under consideration, with the possible exception of Ni. Unfortunately, the values of ζ_{00}, m^*, z, and σ_0 quoted in the literature[23-26] are not consistent with the relations given in Eqs. (15) and (17). However, we note that the most readily available and reliable of these data, namely that for σ_0, can be used to determine a particular combination

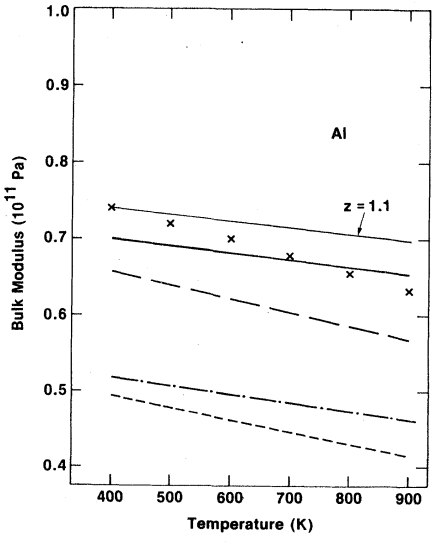

FIG. 8. Bulk moduli of aluminum. Lattice contribution, B_T^l, ---; B_S^l, −·−; lattice plus electron contribution, B_T, ——; $B_S(1)$, ——; $B_S(1.1)$, ——. Experiment (Ref. 20): ×.

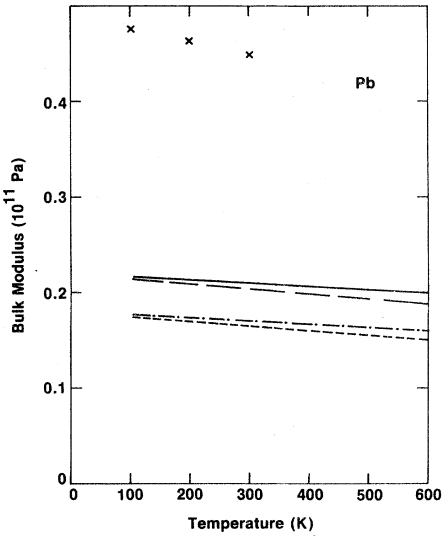

FIG. 9. Bulk moduli of lead. Lattice contribution, B_T^l, ---; B_S^l, $-\cdot-$; lattice plus electron contribution, B_T, ——; B_S, ——. Experiment (Ref. 21): ×.

of parameters, $M' = (m^*/m_0)z^{1/3}$, in terms of which B_T can be expressed, i.e., from Eqs. (15) and (17),

$$M' = \frac{\sqrt{2}\,c}{\pi^2 R k r_0^2}\sigma_0 , \tag{18}$$

where $c = (1/2m_0)(3\sqrt{2}\,h^3N/8\pi)^{2/3}$, m_0 is the free-electron mass, and Eq. (16) becomes

$$B_T^{el} = \frac{2\sqrt{2}\,cz^2}{3M'r^5(T)} . \tag{16'}$$

By this means we avoid the inconsistencies which arise when values of σ_0, ζ_{00}, and z, obtained independently, are used in the calculation. Values of M' are given in Table I. There is still some ambiguity over the value to be used for z, the effective number of electrons per atom, but whatever value we use, the results for B_T^{el} and C_V^{el} will now be obtained consistently in the free-electron picture. In our calculations here we have taken $z = 1$, though we have also investigated the effect of varying z for Al, Pb, and Ni, where we expect z to be different from unity. The computed values of the total bulk moduli B_T and B_S are shown in Figs. 5–10. Since B_S depends on C_P through Eq. (9), we shall leave the discussion of these results until after we have dealt with the specific heat. We just note here that the temperature dependence of B_T enters only through the factor $r^{-5}(T)$. This factor gives a trend similar to that of the available experimental results but it is not strong enough to affect the flattening effect of the factor C_P/C_V on the resulting $B_S(T)$ curve.

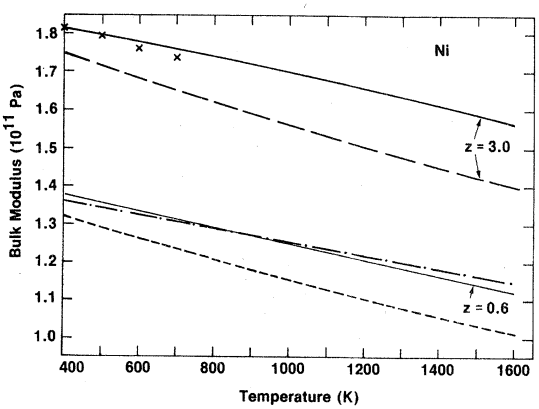

FIG. 10. Bulk moduli of nickel. Lattice contribution, B_T^l, ---; B_S^l, $-\cdot-$; lattice plus electron contribution, $B_S(0.6)$, ——; $B_S(3)$, ——; $B_T(3)$, ——. Experiment (Ref. 22): ×.

C. Specific heat

First of all, we calculated the lattice contribution to C_V and C_P from Eqs. (6)–(8). The results are shown in Figs. 11–16. As expected, C_P^l is less than the experimental values[26] in all cases. The corresponding values for B_S^l, given by Eq. (9), are shown in Figs. 5–10. We now include the electron contribution as described above (Sec. III B). The total isothermal bulk modulus is given by the sum of Eqs. (7) and (16),

$$B_T = \frac{\sqrt{2}\,F''(r,T)}{9r(T)} + \frac{2\sqrt{2}\,cz^2}{3M'r^5(T)} . \tag{19}$$

Equation (8) becomes

$$C_P = C_V^l + \sigma_0 T + \frac{9N}{\sqrt{2}}\alpha^2(T)r^3(T)TB_T , \tag{20}$$

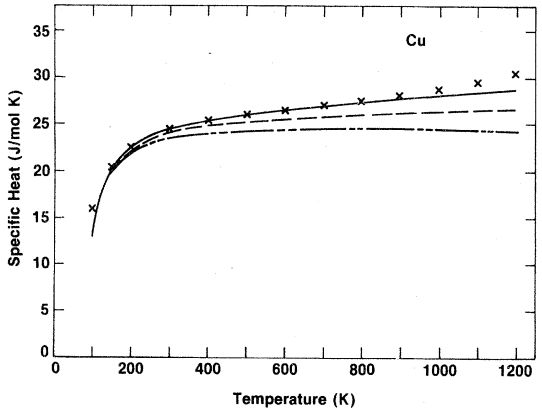

FIG. 11. Specific heat of copper. Lattice contribution, C_V^l, ——; C_P^l, ——; Lattice plus electron contribution, C_P, ——. Experiment: ×. All experimental values of specific heat are taken from Ref. 26. Units are joules per mole Kelvin.

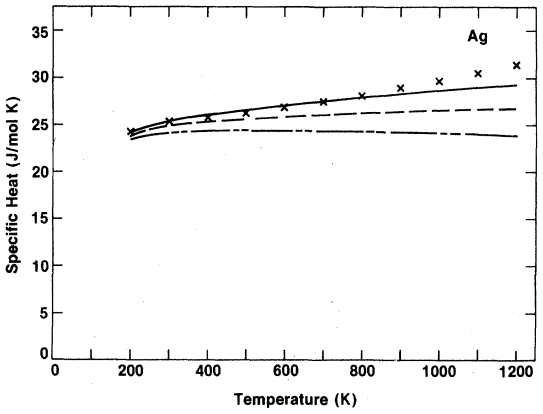

FIG. 12. Specific heat of silver. Lattice contribution, C_V^l, — — —; C_P^l, — —; lattice plus electron contribution, C_P, —. Experiment: ×.

and the total adiabatic bulk modulus is then given by

$$B_S = \frac{C_P}{(C_V^l + \sigma_0 T)} B_T . \tag{21}$$

As we see in Figs. 11–16, C_P is in good agreement with experiment[26] over most of the temperature range considered for each metal. Only in aluminum, nominally trivalent, and nickel, ferromagnetic, is the situation anything less than satisfactory. In aluminum, any significant increase in z above unity makes the bulk modulus (Fig. 8) too large while C_P (Fig. 14), which is much less sensitive to z, is not improved appreciably. In nickel, reduction of z to the quoted value[23] of 0.6 improves the agreement between C_P and experiment but decreases B_S to values comparable to those of the lattice contribution alone. A value of $z = 3$ is needed to bring B_S into agreement with

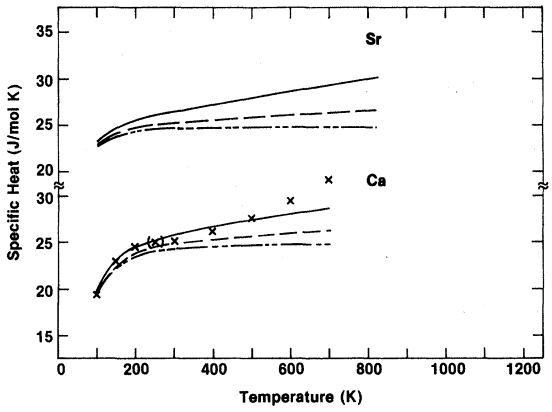

FIG. 13. Specific heat of calcium and strontium. Lattice contribution, C_V^l, — — —; C_P^l, — —; lattice plus electron contribution, C_P, —. Experiment: ×. Note that ordinate is broken.

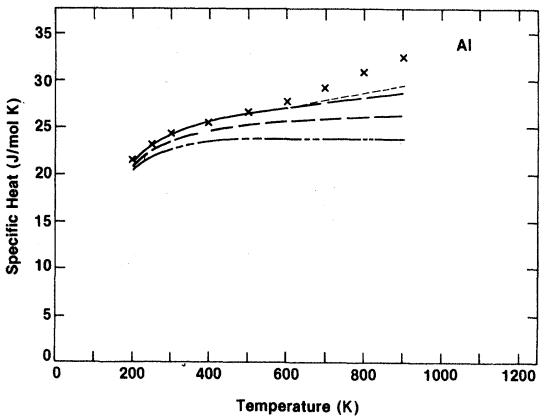

FIG. 14. Specific heat of aluminum. Lattice contribution, C_V^l, — — —; C_P^l, — —; lattice plus electron contribution, C_P, ---; C_P plus vacancy contribution, ----. Experiment: ×.

experiment, but then the values of C_P are too large. We show the effect of varying z in Figs. 10 and 16. Regardless of the value of z, the large value of σ_0 for Ni leads to a predominantly linear dependence of C_P on T, rather than the flattening at high temperatures which is observed experimentally. We note that the situation for lead, nominally quadrivalent, is similar to that for aluminum, although C_P is in very good agreement with experiment when $z = 1$. However, a value of $z = 2.75$ is needed to raise B_S to the experimental level with a consequent increase in the C_P values. Not unexpectedly, this simple treatment of the electrons is inadequate to deal with the more complex electron configurations that obtain in Al, Pb, and Ni. For nickel, in particular, our calculations have not included the magnetic contribution to the specific heat which gives rise to anomalous behavior in the neighborhood of the

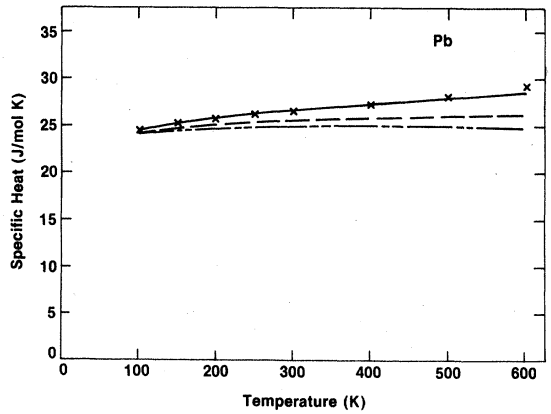

FIG. 15. Specific heat of lead. Lattice contribution, C_V^l, — — —; C_P^l, — —; lattice plus electron contribution, C_P, ---. Experiment: ×.

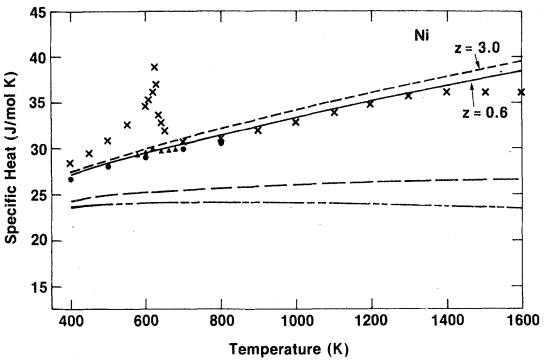

FIG. 16. Specific heat of nickel. Lattice contribution, C_V^l, — — —; C_P^l, — —; lattice plus electron contribution, $C_P(0.6)$, —; $C_P(3.0)$, ---. Experiment: ×. Analyses of Connelly *et al.* (Ref. 4), ▲; Pawel and Stansbury (Ref. 2) ●, (see text).

Curie point (631 K). This contribution has been estimated by Pawel and Stansbury[2] and by Connelly, Loomis, and Mapother.[4] We show their results in Fig. 16; they are in good agreement with ours.

Finally, we consider the vacancy contribution to the specific heat. This is given by the relation

$$C_V^{\text{vac}} = R \exp\left(\frac{s_f}{k}\right)\left(\frac{E_f}{kT}\right)^2 \exp\left(\frac{-E_f}{kT}\right), \tag{22}$$

where s_f and E_f are, respectively, the entropy and energy of formation of a single vacancy. Values of E_f are quite reliable since they can be extracted from the temperature-dependent factor $\exp(-E_f/kT)$ in measured quantities such as the vacancy concentration[17] or the trapping rate of positrons,[27] but the determination of s_f requires accurate knowledge of the absolute value of the equilibrium concentration of single vacancies, and this quantity is less well known. We have used values for E_f and s_f given in a review by Seeger.[28] Values of s_f/k are typically ~0.5; but higher values, ~2.0, are also quoted for aluminum.[17] This amount of variation in s_f/k affects C_V^{vac} by a factor of ~10 and it is only for the higher value of s_f/k that C_V^{vac} is large enough to be visible on the C_P plot (see Fig. 14). A much larger concentration of vacancies would be necessary to account for the observed upward swing in C_P at high temperatures.

D. Grüneisen parameter

For completeness, we have evaluated the Grüneisen parameter

$$\gamma = \frac{3\alpha V B_T}{C_V} = \frac{3\alpha V B_S}{C_P}, \tag{23}$$

a quantity that enters the Mie-Grüneisen form of the equation of state. Insofar as γ departs from a constant value, it provides some measure of the nonharmonic character of the real crystal and, for this reason, it is often used in the analysis of experimental data.[1,3] Table II shows the results we have obtained. In the range of temperature considered here, there is little variation in γ. The calculated values of γ are quite close to the experimental values, except in the case of lead. This is consistent with the particularly low values obtained for B_S in this metal. We also include in Table II values of the reference length $r(293)$, since $r(T)$ rather than $\epsilon(T)$ is needed in our calculations. In all cases, $r(293)$ is in excellent agreement with experiment.

IV. DISCUSSION

We have carried out an exact and consistent calculation of the lattice contribution to the thermodynamic properties of a monatomic fcc crystal in the high-temperature limit, $T > \Theta_D$. We have used a nearest-neighbor central-force model with a modified Morse potential to represent the atomic interactions, and we have applied this model to the metals Cu, Ag, Ca, Sr, Al, Pb, and Ni, using free-electron theory to account for the electrons. We emphasize that, for a given

TABLE II. Grüneisen parameter γ and reference length $r(293)$.

	T (K)	γ	γ_{expt}	$r(293)$ (Å)	$r_{\text{expt}}(293)$ (Å)
Cu	100	1.947	1.994	2.5609	2.5559
	700	2.116	2.021		
	1300	2.127			
Ag	200	2.411	2.378	2.8939	2.8894
	700	2.461			
	1200	2.470			
Ca	200	1.400		3.9520	3.9471
	500	1.417			
	700	1.426			
Sr	100	1.390		4.3079	4.3026
	500	1.420			
	800	1.428			
Al	400	2.150	2.192	2.8717	2.8635
	600	2.162	2.188		
	900	2.146	2.281		
Pb	100	1.260	2.690	3.5062	3.5003
	300	1.270	2.655		
	500	1.275			
Ni	400	1.737	1.892	2.4972	2.4916
	1000	1.714			
	1600	1.660			

substance, the specific form for the pair potential is the sole input to the calculation of the lattice-free energy. This simple model appears to be effective in determining the thermodynamic properties of the system. It should be useful in cases where, for whatever reason, high-temperature experiments have not been carried out, as in Sr, where there are no thermal expansion data above room temperature, and no specific heat data above 20 K. The lattice contribution alone will give a lower limit to the true values and demonstrate the trend to be expected as the temperature increases.

The success of this model for these fcc metals is surprising in view of the wide range of electronic structure (monovalent to ferromagnetic) that they represent. Also, there is the large body of evidence from pseudopotential theory to show that a much longer-range potential is needed for a good interpretation of diverse properties such as the phonon spectrum,[8,9] electrical resistivity,[29] and superconducting transition temperature.[30] It is, of course, perfectly clear that our simple potential must be interpreted as an effective interaction appropriate to the nearest-neighbor model. That it is successful in dealing with the thermodynamic properties of fcc crystals implies that the nearest neighbors dominate the situation and if the environment in which they move is treated satisfactorily, and if the calculations are carried through consistently, then the results will reflect those of the real system under investigation. We emphasize the consistency requirement because care must be taken, when choosing the pair potential, that the potential parameters are also determined from a nearest-neighbor model. Our earlier study[7] showed that one could not use a Morse potential with parameters obtained from an "all-neighbor" fit and expect to get sensible results in a nearest-neighbor calculation of the free energy. We hasten to add that we do not expect this simple nearest-neighbor central-force model to be adequate for dealing with microscopic motions in the system such as defect motions, or with absorption or scattering problems where details of the interaction on a local level are of importance. However, this is not an uncommon feature of empirical potentials. The inconsistencies and pitfalls, as well as the successes, in fitting pair potentials to experimental data, have been well documented.[31] Our work gives an empirical potential that has the advantage of being very simple and, we hope, useful in experimental investigations. Its success provides a powerful incentive to look for a deeper understanding of the model and a derivation of the effective interaction from first principles, for it eventually has to be reconciled with the effective potentials obtained by fits to other types of experimental data, e.g., phonon spectra, elastic constants, and defect energies. We hope that this very interesting and important question will be pursued further.

[1] A. J. Leadbetter, J. Phys. C 1, 1481, 1489 (1968).
[2] R. E. Pawel and E. E. Stansbury, J. Phys. Chem. Solids 26, 757 (1965).
[3] C. R. Brooks, J. Phys. Chem. Solids 29, 1377 (1968); C. R. Brooks and R. E. Bingham, *ibid.* 29, 1553 (1968).
[4] D. L. Connelly, J. S. Loomis, and D. E. Mapother, Phys. Rev. B 3, 924 (1971).
[5] R. C. Shukla and C. A. Plint, Int. J. Thermophys. 1, 299 (1980).
[6] R. C. Shukla, Int. J. Thermophys. 1, 73 (1980).
[7] R. C. Shukla and R. A. MacDonald, High Temp. High Pressures 12, 291 (1980).
[8] M. Rasolt and R. Taylor, Phys. Rev. B 11, 2717 (1975).
[9] S. Prakash and P. Lucasson, Phys. Rev. B 17, 1700 (1978).
[10] A. A. Maradudin, P. A. Flinn, and R. A. Coldwell-Horsfall, Ann. Phys. (N.Y.) 15, 360 (1961).
[11] R. C. Shukla and R. Taylor, Phys. Rev. B 10, 4116 (1974).
[12] Y. S. Touloukian, R. K. Kirby, R. E. Taylor, and P. D. Desai, in *Thermal Expansion, Metallic Elements and Alloys*, Vol. 12 of *TPRC Series on Thermophysical Properties of Matter*, edited by Y. S. Touloukian and C. Y. Ho (Plenum, New York, 1975).
[13] T. A. Hahn, J. Appl. Phys. 41, 5096 (1970); R. K. Kirby (private communication).
[14] P. J. Davis and I. Polonsky, in *Handbook of Mathematical Functions*, edited by M. Abramowitz and I. A. Stegun, Natl. Bur. Stand. Appl. Math. Ser. No. 55 (U. S. GPO, Washington, D. C., 1964), p. 914.
[15] Y. P. Varshni and F. J. Bloore, Phys. Rev. 129, 115 (1963).
[16] F. Seitz, *Modern Theory of Solids* (McGraw-Hill, New York, 1940), p. 3.
[17] R. O. Simmons and R. W. Balluffi, Phys. Rev. 117, 52 (1960); 129, 1533 (1963).
[18] Y. A. Chang and R. Hultgren, J. Phys. Chem. 69, 4162 (1965).
[19] J. R. Neighbours and G. A. Alers, Phys. Rev. 111, 707 (1958).
[20] D. Gerlich and E. S. Fisher, J. Phys. Chem. Solids 30, 1197 (1969).
[21] D. L. Waldorf and G. A. Alers, J. Appl. Phys. 33, 3266 (1962).
[22] G. A. Alers, J. R. Neighbours, and H. Sato, J. Phys. Chem. Solids 13, 40 (1960).
[23] J. C. Slater, *Introduction to Chemical Physics* (McGraw-Hill, New York, 1939).
[24] C. Kittel, *Introduction to Solid State Physics* (Wiley, New York, 1956).
[25] A. H. Wilson, *The Theory of Metals* (Cambridge University Press, Cambridge, 1954).

[26]R. Hultgren, P. D. Desai, D. T. Hawkins, M. Gleiser, K. K. Kelley, and D. D. Wagman, *Selected Values of Thermodynamic Properties of Metals and Alloys*. (American Society for Metals, Cleveland, 1973).
[27]A. Seeger, J. Phys. F 3, 248 (1973).
[28]A. Seeger, Cryst. Lattice Defects 4, 221 (1973).
[29]R. C. Shukla and R. Taylor, J. Phys. F 6, 531 (1976).
[30]J. P. Carbotte and R. C. Dynes, Phys. Lett. 25A, 685 (1967).
[31]R. Taylor, *Symposium on Interatomic Potentials and Computer Simulation of Defects in Metals*, TMS-AIME Fall Meeting, Pittsburgh, 1980 (in press).